Astron. Astrophys. 353, 177–185 (2000)

ASTRONOMY AND ASTROPHYSICS

A systematic analysis of X-ray variability of dM stars

A. Marino[1], **G. Micela**[1], **and G. Peres**[2]

[1] Osservatorio Astronomico G.S. Vaiana, Piazza del Parlamento 1, 90134 Palermo, Italy (marino, gmicela@oapa.astropa.unipa.it)
[2] Dipartimento di Scienze Fisiche e Astronomiche, Università di Palermo, Piazza del Parlamento 1, 90134 Palermo, Italy (peres@oapa.astropa.unipa.it)

Received 24 November 1998 / Accepted 11 October 1999

Abstract. We have systematically analyzed X-ray variability of dM stars. Our data base is the sample of all dM stars listed in the CNS3 (Gliese & Jahreiss 1991) catalog which have been observed with the ROSAT PSPC.

Our data sample includes 86 pointed observations of 55 distinct stars or multiple systems. A large fraction of stars shows significant variations, regardless of their quiescent flux. Variability is detected on all observable time scales. The amplitudes of these variations are independent of both stellar X-ray and visual luminosity. Compared to solar X-ray variability properties our results suggest that the amplitude distribution of X-ray variability in dM stars is consistent with the analogous distribution for solar flares.

We discuss the effect of variability on the spread observed in the X-ray luminosity function of M stars.

The comparison of our data with those obtained with *Einstein IPC* shows that variations on time scales shorter than a few month are more common than long term variations comparable to, e.g., the 11 years solar cycle.

Key words: stars: coronae – stars: late-type – X-rays: stars – Galaxy: solar neighbourhood

1. Introduction

X-ray variability studies are a powerful tool to study coronal X-ray emitters. Analyses of larger samples of stars may provide typical time scales and amplitudes for the observed variability. This is important information on dimensions and physical conditions of the regions where X-ray emission originates and, in principle, allows us to infer on the mechanisms responsible for the observed emission. Generally speaking, the X-ray variability properties of an homogeneous class of stellar X-ray emitters allow us to constrain the X-ray generating mechanisms in these stars. To pursue such studies, a large number of homogeneous observations are required.

Prior to the launch of the *Einstein* Observatory in 1978 (Giacconi et al. 1979), only a few examples of stellar coronal X-ray emission were known. Observations with the *Einstein* Observatory have shown the ubiquity of stellar coronal X-ray emission throughout the HR diagram (Vaiana et al. 1981). Together with data obtained during later missions X-ray variability of stellar coronal emission can be investigated on time scales ranging from several minutes to a couple of years for a large sample of data.

Using *Einstein* and EXOSAT (White & Peacock 1988) data, systematic studies of X-ray emission variability were made on various samples of stars (e.g. Montmerle et al. 1983, Ambruster et al. 1987, Collura et al. 1988, Pallavicini et al. 1990). Most of the *Einstein* observations were of short duration (typically a few thousand seconds each), with many sources being observed only once. Moreover gaps in the *Einstein* data, due to the low orbit of the satellite, make the determination of the time scale distribution of the variations rather difficult and hence to infer the nature of the observed variability. In the case of X-ray observations of the same source taken with different instruments uncertainties may arise from a cross-calibration of the data. Even when using a single instrument, it is difficult to disentangle short-term variations due to flares from more gradual variations caused by star rotation and/or by stellar activity cycles.

So far the Sun is the only star for which X-ray variability is intensively studied on virtually all time scales (e.g. Vaiana et al. 1973, Vaiana & Tucker 1974, Kreplin et al. 1977, Zombeck et al. 1978, Withbroe et al. 1985). The soft X-ray emission of the Sun is highly variable on time scales ranging from minutes to years. Variations observed in the spatially integrated solar X-ray flux can be directly related to the spatial emission distribution observed in the high-resolution X-ray images of the Sun. Since no equivalent studies are possible for other stars, X-ray variability studies provide a powerful tool to test origin and properties of coronae of late-type stars.

dM stars are the most numerous stars in the Galaxy. For these stars variability has been observed at all wavelengths and it suggests that their atmospheres are very dynamic. Systematic investigations of variability in the coronal X-ray emission from dM and dMe stars have been performed with *Einstein* and the EXOSAT data. Ambruster et al. (1987) have shown that short-time variability (from several minutes to hours), with a typical amplitude of 30–50% is common in M stars. The continuous time coverage of EXOSAT has confirmed the presence of flaring activity superimposed on quiescent emission also highly

Send offprint requests to: G. Micela (gmicela@oapa.astropa.unipa.it)

variable on these stars (Collura et al. 1988, Pallavicini et al. 1990).

In this paper we present a systematic study of X-ray variability of nearby M stars detected in ROSAT PSPC (Pfeffermann et al. 1987, Trümper 1992) pointed observations. ROSAT observations (similary to *Einstein* ones) are fragmented in time segments of typically a few thousand seconds. However, the sensitivity of ROSAT PSPC is much higher than that of the *Einstein* IPC, thus allowing us to study variability of smaller amplitudes and in more X-ray quiet stars. Furthermore, a better time coverage is given since the typical observation live times with ROSAT are longer than with *Einstein*.

Our paper is organized as follows: in Sect. 2 we present our sample of dM stars, the X-ray data, and their analysis. The basic results are given in Sect. 3. In Sect. 4, we draw our conclusions.

2. Observations and data analysis

2.1. The sample

Our sample contains all dM stars, within 25 pc, listed in the CNS3 catalog, and which have been detected in ROSAT PSPC pointed observations. Among these we have selected all stars detected with more than 40 net counts and having an off-axis angle from the center of the field of view ≤48 arcmin. Our sample consists of 55 stars, for a total of 86 distinct observations. Sixteen of these stars were multiply observed with the ROSAT PSPC at time intervals typically separated by months. In these cases we can explore variability properties up to these time scales. Table 1 summarizes the optical and kinematical characteristics of our sample stars. Column 1 provides the stellar names according to the catalogs by Gliese & Jahreiss, Woolley or the CNS3 catalog, while more common names are given in Column 7. The other data are taken from the CNS3 catalog. Classification in terms of young disk - old disk - halo (YD-OD-H) kinematic population given in Column 5 is from Leggett (1992).

2.2. X-ray observations

Table 2 provides a journal of the ROSAT PSPC observations used in our study. Column 1 gives the star's name (as in Table 1). The ROSAT Observation Request (ROR) is listed in Column 2, and the date of the ROSAT PSPC observation in Column 5. The exposure-time for each observation is given in Column 3, while in Column 4 we provide the length of the observation. In Column 6 we give the hardness ratio and in Column 7 the count rate. The mean X-ray luminosity, computed as explained below, is given in Column 8 and the results of the Kolmogorov-Smirnov test (e.g. Eadie et al. 1971, Siegel 1956) are presented in Column 9. The presence of evident flares is indicated in Column 10.

For each star we evaluated the number of counts in a circular region centered on the average position of the observed photons in the (0.1–2.4) keV range and with radius R, ranging from 2 arcmin, for sources positioned on the axis, up to 5 arcmin, for sources at large off-axis positions. Count rates of the off-axis sources were corrected for vignetting. The radius R has been determined from the radial profile of the spatial

Table 1. Optical properties of the selected sample

Name	Sp. Type	Dist. (pc)	Mv	POP.	Single Bin./Triple	Other name
GL1	M4	4.51	10.27	H	S	HD225213
GL26	M4	12.59	10.56		S	LHS119
GL46	M3.5	13.95	11.05		S	LHS129
GL54.1	M5e	3.74	14.19	OD	S	LHS138
GL65A	M5.5e	2.63	15.47	YD	B	UV Ceti
GL65B	M5.5e	2.63	15.60	YD	B	UV Ceti
GL70	M2	8.79	11.21		S	LHS1290
GL169.1A	M4	5.50	12.38	OD	B	LHS26
CNS783	k-m	15.87	13.60		S	
GL182	M0.5	18.90	9.02	YD	S	
GL191	M0 V	3.87	10.91	H	S	Kapteyn's star
GL195A	M2	13.11	9.61	YD	B	
GL195B	M4	13.11	9.61	YD	B	
GL205	M1.5	5.80	9.14	OD	S	LHS30
GL206	M4e	14.10	10.77	YD	S	
GL213	M4	6.01	12.64	O/H	S	Ross 47
GL251	M4	5.76	11.21	Y/O	S	
GL274B[1]		16.92	11.40		B	
GL294C[1]		15.87	12.50		T	
GJ1111	M6.5	3.63	17.01	YD	S	LHS248
GL316.1	m	15.50	16.70		S	LHS2034
GJ1114	M2	16.39	10.47		S	LHS2060
GL354.1	m	18.66	15.10		S	
GL360	M3	13.50	9.92	YD	S	LHS2176
GL388	M4.5e	4.90	10.95	YD	S	AD Leo
GL398	M4e	13.70	11.92		S	RY Sex
CNS1673	m	4.49	15.66		S	LHS288
GL406	M6	2.39	16.56	OD	S	CN Leo
GL410	M2e	11.00	9.39	Y/O	S	
GL411	M2e	2.52	10.48	OD	S	HD95735
GL447	M4.5	3.32	13.51	OD	S	LHS315
GL473A	M5.5e	4.31	14.87	YD	B	LHS333
GL473B	M7	4.31	15.10	YD	B	
GL490A	M0 Ve	21.10	9.06		B	
GL490B	M4e	21.10	11.58		B	
GL494	M1.5e	11.12	9.52	YD	S	DT Vir
GL505B[1]	M1 V	11.90	9.20		B	LHS2714
GL551	M5e	1.30	15.49	Y/O	S	PROX Cen
GL615.2	M3.5	22.52	10.55	S		
GL625	M2	6.28	11.13	YD		
GL630.1	M4e	14.49	12.09	H	B	CM Dra
GL643	M4	5.82	12.98	OD	S	LHS427
GL644A	M3	6.50	10.63	OD	T	Wolf 630
GL644B		6.50	10.80	OD	T	Wolf 630
GL644C	M7	6.50	17.72	OD	T	VB8
GJ1207	M3.5	9.58	12.37		S	LHS3255
GL687	M3.5 V	4.70	10.82	OD	S	LHS450
GL695B[1]	M3	8.69	10.66		T	LHS3325
GL695C[1]	M4	8.69	11.10		T	
GL699	M5 V	1.83	12.23	O/H		Barnard's star
Wo9615		20.58	12.00			
GL725A	M4	3.50	11.18	Y/O	B	LHS58
GL725B	M5	3.50	11.99	Y/O	B	LHS59
GL752A	M3.5e	5.66	10.35	OD	B	LHS473
GL752B	M5e	5.66	18.76	OD	B	LHS474
GL783B[1]	M3.5	5.65	12.70		B	LHS486

Table 1. (continued)

Name	Sp. Type	Dist. (pc)	Mv	POP.	Single Bin./Triple	Other name
GL821	M3	10.91	10.68	H	S	Wolf 918
GL832	M1 V	4.65	10.33	OD	S	LHS3685
GL866AB	M5e	3.40	15.00	OD	B	L798-6
GL873	M4.5e	5.08	11.73	Y/O	S	EV Lac
GL875.1	M3.5e	15.38	10.69	YD	S	GT Peg
GL876	M5	4.73	11.79	YD	S	LHS530
GL887	M2 Ve	3.52	9.61	OD	S	HD217987
GL897A	M3.5	12.90	10.40		T	
GL897B		12.90	10.40		T	

[1] These stars are part of multiple systems with different spectral type stars.

photons distribution of each source: R is the distance measured from the centroid of the source where the photon density drops to a fraction f with respect at the centroid density. We have chosen a different fraction f for sources with different statistics. In particular, defining η the number of photon counts per pixel at the centroid (1 pixel =5″), we have chosen $f = 10^{-5}$, 10^{-4}, $3{\cdot}10^{-2}$ for $\eta > 1$, $1 \geq \eta > 0.1$, and $\eta \leq 0.1$, respectively. The background was measured in an annulus, between R+25 arcsec and R+50 arcsec, centered on the centroid of the source. In some cases we had to perform "pie cuts" to exclude contributions from nearby intense sources.

2.3. Flux and luminosity determination

The conversion factor from count rate to X-ray flux depends on the instrumental properties, the interstellar hydrogen column along the line of sight, and the source spectrum. The X-ray emission was assumed to be produced by a single temperature plasma described by a Raymond-Smith model spectrum (Raymond & Smith 1977). Interstellar absorption has not be included since this effect is negligible in the case of our sample of nearby stars. For these conditions we modeled a conversion factor [erg cm^{-2}/count] as a function of the observed Hardness Ratio (HR= $\frac{H-S}{H+S}$), S being the number of photons measured in channels 3–10 (0.11–0.42 keV) and H the photon number recorded in channels 11–30 (0.42–2.4 keV) (see also Schmitt et al. 1995). In Fig. 1 we show the result. The Hardness Ratio is a non-monotonic function of temperature; for HR< 0 (T $\lesssim 0.25$ keV) the relation between conversion factor and HR is single valued, however, for HR> 0 the relation is double valued. For our sample stars with HR> 0 we adopted the lower conversion factor. The systematic error in the derived fluxes is of the order of 15%.

We computed X-ray luminosities employing the obtained fluxes and distances reported in the CNS3 catalog. Since each observation consists of a set of temporal segments obtained during different satellite orbits we estimated count rate, HR, flux and X-ray luminosity for each temporal segments with at least 30 counts.

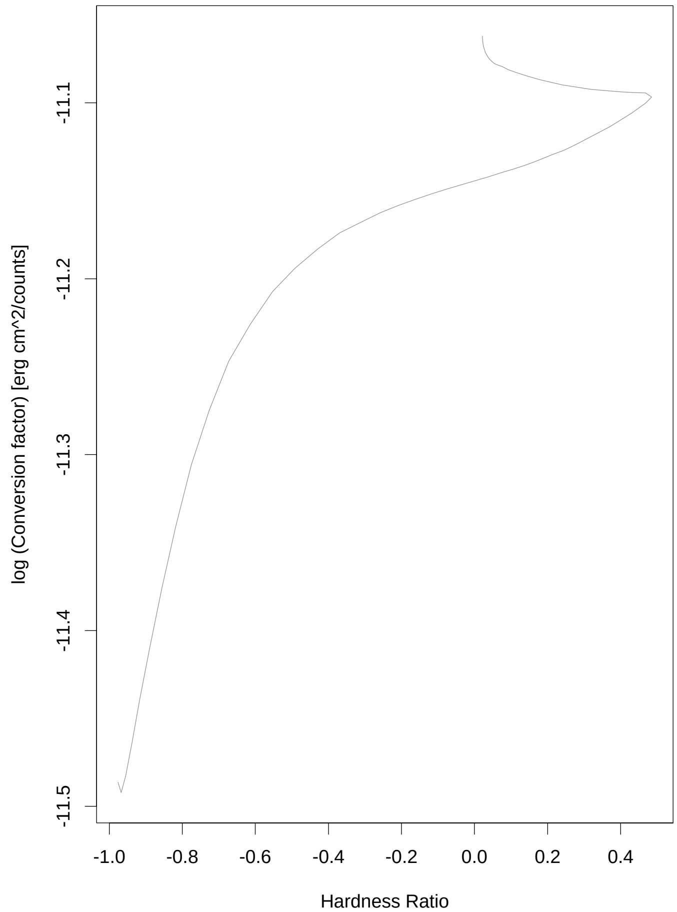

Fig. 1. Conversion factor from count rate to flux, for Raymond thermal spectrum convolved with the instrumental spectral response, vs. the Hardness Ratio.

3. Results

3.1. Time variability

For each star in our sample, we obtained light curves in the 0.11–2.4 keV band. Variability is present on many time scales and does not appear to depend on X-ray luminosity. Fig. 2 shows examples of light curves of stars with typical X-ray luminosity ranging within two orders of magnitude ranging from 3×10^{27} for GL866 to 3×10^{29} erg/sec for GL490. As it can be seen, variability does not depend on X-ray luminosity. This finding will be discussed in more detail below.

For a statistical evaluation of the X-ray variability we applied the unbinned Kolmogorov-Smirnov (K-S) test to the X-ray light curves of our sample stars. We used the procedure implemented in the pros.xtiming package of IRAF with data gaps removed. This method does not allow us to distinguish stochastic variability or other forms of variability from periodic ones (see also Collura et al. 1987 and Haisch & Schmitt 1994 for a more sophisticated treatment of the gaps).

For each observation, we ran the K-S test on the source counts as well as the counts detected in the background regions. The latter has been carried out to monitor possible background variability. In only three cases the background is variable on

Table 2. Journal of ROSAT PSPC observations. Asterisks indicate stars with at least four temporal segments having more than 30 counts each, as used in Sect. 3.2.

Name	Obs.seq.	Exposure Time (s)	Elapsed Time (s)	Observing Dates	HR	Rate ± Err. [cnt/s]	L_x [erg/s]	Results of the K-S test	Notes
GL1	201008	4804	30411	30/11/92	-0.62	0.022 ± 0.002	26.50	$90\% - 95\%$	
GL26*	201045	28366	523978	22-28/7/92	-0.59	0.017 ± 0.001	27.33	$95\% - 99\%$	Flare?
GL46*	700528a01	12516	511859	8-14/12/92	-0.46	0.008 ± 0.001	27.14	≤90%	
GL46*	700528	18200	970628	4-15/6/92	-0.46	0.019 ± 0.001	27.50	≥99%	Flare
GL46*	701223	48943	411073	3-8/7/92	-0.24	0.0068± 0.0004	27.10	$90\% - 95\%$	
GL54.1	201104	1408	6506	10/7/92	-0.70	0.085 ± 0.008	26.89	$95\% - 99\%$	
GL65AB*	200208	25814	1322203	30/12/91-15/1/92	-0.23	0.724 ± 0.005	27.78	≥99%	Flare
GL70	200468	8548	405414	26-31/1/92	-0.47	0.035 ± 0.002	27.32	$95\% - 99\%$	Flare?
GL169.1A	201114	3513	6342	21/8/92	-0.87	0.011 ± 0.002	26.22	≤90%	
CNS783*	900353	7724	225124	21-24/2/93	-0.13	0.033 ± 0.002	27.97	$90\% - 95\%$	
CNS783*	200443	20074	262364	7-10/3/91	-0.02	0.022 ± 0.001	27.80	≥99%	Flare
CNS783*	201313	4033	12920	10/9/92	-0.04	0.045 ± 0.003	28.18	≥99%	Flare
GL182*	200118	5942	13643	22/2/91	-0.13	0.813 ± 0.012	29.39	≥99%	
GL182*	200517	3380	92971	24-25/2/92	-0.11	0.77 ± 0.015	29.37	≥99%	Flare
GL182*	200517a01	1806	1806	16/2/93	-0.17	0.50 ± 0.017	29.18	≤90%	
GL191*	200523	14994	76152	31/3/92-1/4/92	-0.74	0.029 ± 0.001	26.43	≥99%	
GL191*	201105	3056	150297	29/9/92-1/10/92	-0.63	0.055 ± 0.004	26.76	$95\% - 99\%$	
GL195AB*	200657	2418	248166	24-27/3/92	-0.34	0.082 ± 0.006	28.25	≤90%	
GL195AB*	200799	9436	89097	11-12/3/92	-0.21	0.143 ± 0.004	28.51	≥99%	
GL205*	200036	7528	191316	13-15/3/91	-0.36	0.131 ± 0.004	27.63	≥99%	
GL206*	200200a00	212	212	27/3/91	-0.09	3.76 ± 0.13	30.00	≤90%	
GL206*	200200a01	2134	2137	27-28/3/92	-0.33	0.379 ± 0.013	28.99	≤90%	
GL206*	201026	5073	10500	22/9/92	-0.33	0.375 ± 0.009	28.96	≥99%	
GL213	201338	14026	289782	21-25/9/92	-0.70	0.006 ± 0.001	26.15	≤90%	
GL251	201116	4150	174372	30/9/92-2/10/92	-0.52	0.011 ± 0.002	26.45	≤90%	
GL274	800348	4080	7933	10/4/93	-0.12	0.189 ± 0.007	28.86	$90\% - 95\%$	
GL294*	200668	9156	156575	6-8/4/92	-0.94	0.014 ± 0.001	27.28	≤90%	
GL294*	201754	27146	271234	25-28/9/93	-0.71	0.027 ± 0.001	27.74	≤90%	
GL294*	20175401	33651	673719	6-13/12/93	-0.60	0.034 ± 0.001	27.89	≤90%	
GL294*	201754a02	16995	486180	30/4/94-5/5/94	-0.45	0.043 ± 0.002	28.03	≥99%	Flare
GJ1111*	200453	15727	121972	10-12/4/91	-0.47	0.035 ± 0.001	26.72	≥99%	Flare
GL316.1	200607	1638	1638	25/4/93	-0.11	0.030 ± 0.004	27.84	≤90%	
GL316.1	200620	1438	161508	12-14/11/91	-0.04	0.312 ± 0.015	29.04	≥99%	
GJ1114	700541	6003	13452	27-28/4/92	-0.23	0.050 ± 0.003	28.16	≥99%	Flare
GL354.1	201506	2221	2317	31/10/93	-0.14	0.725 ± 0.018	29.33	≤90%	
GL360*	600516	8126	167446	7-9/10/91	-0.24	0.152 ± 0.004	28.59	≥99%	Flare
GL388*	200076	15242	87909	8-9/9/91	-0.13	3.941 ± 0.016	28.90	≥99%	Flare
GL398	201724	202	648	4/12/93	0.02	0.206 ± 0.032	28.52	≤90%	
CNS1673	201580	760	760	21/7/93	-0.37	0.188 ± 0.016	27.48	≤90%	
GL406	201577	1493	1493	4/12/93	0.04	1.018 ± 0.026	27.70	≥99%	Flare
GL406	201722	2684	7500	4-5/12/93	-0.16	0.273 ± 0.010	27.12	≥99%	
GL410*	200987	5027	644298	2-9/6/93	-0.21	0.182 ± 0.006	28.26	≥99%	
GL411*	200127	10389	168374	26/5/91-7/5/92	-0.66	0.235 ± 0.005	27.01	≥99%	
GL447	201242	5837	500005	23-28/6/92	-0.50	0.052 ± 0.003	26.97	$95\% - 99\%$	Flare?
GL473AB	201112	646	646	7/7/92	-0.36	0.247 ± 0.020	27.57	≤90%	
GL473AB	201112a01	1994	1994	19/6/93	-0.27	0.297 ± 0.012	27.66	≥99%	
GL490AB*	600164	16752	311049	20-24/12/91	-0.20	0.568 ± 0.006	29.43	≥99%	Flare
GL490AB*	701118	4054	13701	31/12/92	-0.18	0.624 ± 0.012	29.37	≥99%	
GL494*	400116	8303	93461	17-18/12/91	-0.17	0.613 ± 0.009	29.03	≥99%	Flare
GL494*	200515a00	3180	30657	23/12/91	-0.19	0.943 ± 0.017	28.99	≥99%	
GL494*	200515a01	1706	1706	14/6/92	-0.13	1.205 ± 0.027	29.10	≤90%	
GL505	201372	1708	6068	11/7/92	-0.42	0.224 ± 0.011	28.40	≤90%	
GL551*	200646a01	374	374	17/8/93	-0.06	1.106 ± 0.054	27.20	≥99%	
GL551*	200502	3943	706236	1-10/3/92	-0.30	0.878 ± 0.015	27.08	≥99%	
GL551*	200502a01	7854	442115	4-9/2/93	-0.47	0.612 ± 0.009	26.90	≥99%	

Table 2. (continued)

Name	Obs.seq.	Exposure Time (s)	Elapsed Time (s)	Observing Dates	HR	Rate ± Err. [cnt/s]	L_x [erg/s]	Results of the K-S test	Notes
GL551*	200502a02	20294	167553	27-29/8/93	-0.39	0.581 ± 0.005	26.89	≥99%	Flare
GL551*	200502a03	3833	239626	27/2/94-10/3/94	-0.37	1.054± 0.017	27.15	≥99%	Flare
GL615.2*	200919	5780	42377	16/1/93	-0.27	0.035± 0.002	28.18	$90\% - 95\%$	
GL615.2*	200438	4267	202421	30/8/92-1/9/92	-0.14	0.036 ± 0.003	28.19	≤90%	
GL615.2*	700842	3651	139182	30-31/8/92	-0.69	0.017 ± 0.002	27.86	≤90%	
GL625	201582	7487	174125	22-24/9/93	-0.38	0.027 ± 0.002	26.92	≥99%	Flare
GL630.1*	200721	47465	334715	1-5/4/92	-0.26	0.132 ± 0.002	28.36	≥99%	Flare
GL643-644AB*	200125	8780	161672	25-27/2/91	-0.23	3.482 ± 0.020	28.54	≥99%	
GL644C*	200125	8780	161672	25-27/2/91	-0.12	0.098 ± 0.003	28.43	≥99%	Flare
GJ1207*	4000388	9420	36483	1-2/9/93	-0.21	0.367 ± 0.006	28.55	≥99%	
GL687*	9999995	6427	5834896	27/2/94-5/5/94	-0.54	0.073 ± 0.003	27.08	≥99%	Flare
GL687*	999995a01	4129	3078099	31/5/94-6/7/94	-0.54	0.065 ± 0.004	27.03	$95\% - 99\%$	
GL695AB	201126	608	606	6-7/4/93	-0.73	0.158 ± 0.016	27.88	≤90%	
GL699	200128	4515	34705	3/5/91	-0.89	0.023 ± 0.002	25.57	$90\% - 95\%$	Flare
Wo9615	201764	10317	46805	8/9/93	-0.42	0.019 ± 0.001	27.97	≤90%	
GL725AB	201135	2365	2365	28/11/92	-0.77	0.065±0.005	26.68	≤90%	
GL752AB	200126	7280	521172	26/3/91-5/4/91	-0.67	0.033 ± 0.002	26.85	≤90%	
GL783	201581	1995	448378	9-14/10/93	-0.78	0.029 ± 0.004	26.74	≤90%	
GL821	201007	18215	689568	25/4/93-3/5/93	-0.52	0.006 ± 0.001	26.76	≤90%	
GL832	201110a01	2152	7455	13-14/4/93	-0.96	0.037 ± 0.004	26.49	≤90%	
GL866*	201723	13203	47260	7/12/93	-0.35	0.333 ± 0.005	27.49	≥99%	Flare
GL873*	200984	2675	350752	13-17/7/92	-0.07	10.875± 0.064	29.38	≥99%	Flare
GL873*	201587	7755	18440	12-13/7/93	-0.29	1.131 ± 0.012	28.57	≥99%	
GL873*	201586	5934	18116	11-12/7/93	-0.33	1.190 ± 0.014	28.59	≥99%	
GL873*	201585	4563	16512	10-11/7/93	-0.30	1.076 ± 0.015	28.54	≥99%	
GL873*	201584	3858	16459	9-10/7/93	-0.26	1.414 ± 0.019	28.67	≥99%	
GL873*	201583	3445	12553	8-9/7/93	-0.22	1.462 ± 0.021	28.68	≥99%	
GL875.1	200986	3622	46945	23/6/92	-0.23	0.337 ± 0.010	28.82	≥99%	
GL876	201111	1812	1812	27/5/93	-0.50	0.024 ± 0.004	26.62	≤90%	
GL887*	201339	13588	841111	4-5/6/93	-0.55	0.240 ± 0.004	27.35	≥99%	Flare
GL897AB	201124	858	858	24/5/93	-0.20	0.693 ± 0.028	28.98	$90\% - 95\%$	

confidence level $> 99\%$. However, in these cases, the number of counts in the variable background is much lower than the counts attributed to the source, hence leading to reliable test results for these sources. In Column 9 of Table 2 we report the results in terms of the confidence level at which we can reject the hypothesis that the source in the given observation is constant.

Obviously, the sensitivity to variability depends on statistics and those sources found to be variable show, on average, more counts than other sample stars with a lower significance level for variability. In particular, we find that 29 out of 32 sources observed with more than 1000 net counts are variable at a significance level greater than 99%. This finding suggests that all dM stars are X-ray variable and the detection of variability is only limited by photon statistics.

In several cases we cannot determine the characteristics and properties of the variability because of temporal gaps in the data, time decay or the characteristic time of the observed variations then cannot be measured.

In Table 3 we present a summary of our K-S test results, separately for stars with $M_v \leq 13$ and $M_v > 13$: at $M_v \approx 13$ stellar structure models predict that stars become fully convective and then are unable to support a magnetic dynamo (Golub 1983, Rosner et al. 1985, Durney et al. 1993). The table indicates that variability is common both in the brightest and in the faintest stars, thus indicating no significant change in X-ray variability properties at $M_v \approx 13$.

Analogously Table 4 reports our K-S results for stars of different X-ray luminosities. These results confirm again that for stars with $L_x > 10^{27}$ erg/s variability is independent of L_x. We also note that stars with $L_x < 10^{27}$ erg/s yielded the lowest number of photon counts. In particular, 6 out of the 9 stars with significance less than 90% have less than 100 counts. If we consider only the stars of this subsample with high statistics, we find that the frequency of the variable sources is similar to that of the other more luminous subsample. We conclude that X-ray variability is a general property of dM stars, independent of the quiescent value of the L_x.

We have also applied a χ^2 test, to our light curves, obtaining equal or less significant variability. We think that the difference between the results obtained with K-S and χ^2 tests is due to the binned nature of the χ^2 test. In general, binning leads to a loss of information (cf. Siegel 1956); in our investigation we used

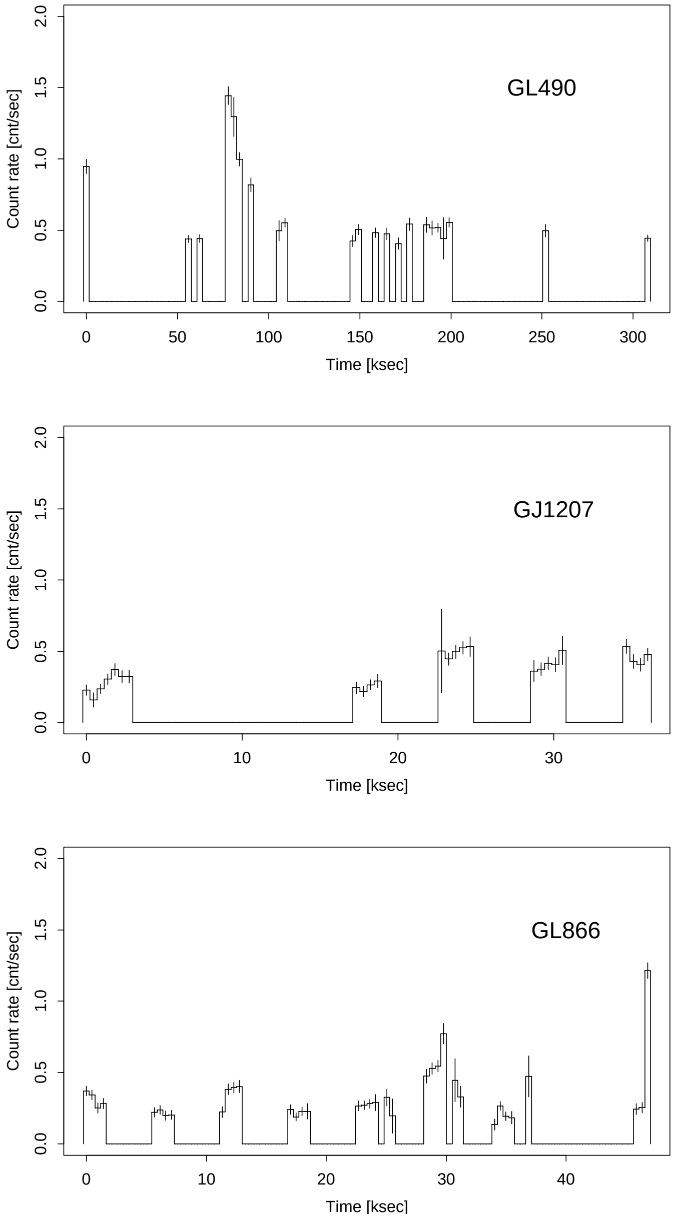

Fig. 2. Examples of light curves of stars with very different typical X-ray luminosity, from top to bottom: GL490 ($L_x = 3 \cdot 10^{29}$), GJ1207 ($L_x = 3 \cdot 10^{28}$), and GL866 ($L_x = 3 \cdot 10^{27}$).

the unbinned version of the K-S test. Attempts to overcome the binning-related problem of the χ^2 test have been made in the past (Collura et al. 1987) modifying the classical test so as to phase shifts and the time scale of the binning. In our case, the low number of photon counts of most of our sources imply that a more detailed analysis cannot improve our results.

3.2. Time X-ray distribution function

In the following we investigate the cumulative time luminosity function (in the following Time XLD), i.e., the luminosity distribution function of all time segments in an observation. It allows us to evaluate the statistical characteristics of the observations.

Table 3. Results of the K-S test for the stars with $M_v \leq 13$ and $Ms_v > 13$.

Results of the K-S test	Number of stars with $M_v \leq 13$	Number of stars with $M_v > 13$
>99%	31	14
95%-99%	4	2
90%-95%	6	1
≤90%	24	4

Table 4. Results of the K-S test for different ranges of the mean L_x.

	L_x			
Results of K-S test	$< 10^{27}$	$10^{27} - 10^{28}$	$10^{28} - 10^{29}$	$\geq 10^{29}$
>99%	5	14	20	6
95%-99%	4	2	0	0
90%-95%	2	2	3	0
≤90%	9	10	5	4

We have constructed the Time XLD for the 27 stars of our sample (indicated by an asterisk in Table 2) which have at least four temporal segments with more than 30 counts each. We have eliminated data points with a large error in the conversion factor (due to a large error in HR) because the X-ray luminosity is essentially undetermined in these cases. The resulting distribution gives us the fraction of time in which the X-ray luminosity is greater than a given value.

In order to test whether the observed spread in time distribution is an intrinsic property of the star or the result of statistic fluctuations we made the following simulations: assuming that the star has a constant luminosity corresponding to the minimum value observed, we computed the net counts expected $c_{\rm exp,i}$ in each of the N temporal segments of the observations. We generated a set of simulated data from the N Poisson distribution centered on $c_{\rm exp,i}$, that represents a possible outcome from the observations if the source has a constant luminosity corresponding to the minimum value observed. For each star we generated 100 of such simulations to evaluate the spread in the Time XLD introduced by statistical fluctuations. The results was then compared to the observed spread. The fraction of the observed variance that can be explained by statistical fluctuations is generally small. Table 5 shows the number of cases for which a given percentage of the observed variance is due to statistical fluctuations.

For the sample stars GL873, GL65, and GL551 Fig. 3 shows the observed Time XLD (single line to the right) and the simulated Time XLD function (lines to the left). In all three cases the observed Time XLD appears to the right of the simulated one. This demonstrates that for these stars statistical fluctuations account only for, at most, 1% of the observed variance, thus indicating that the spread of the distribution function is real. We note that the choice of the minimum observed value as the "true" value for the X-ray quiescent luminosity of the star, can shift the simulated curve along the L_x axis, but has only a little effect on the spread in the Time XLDs. Note that the spread

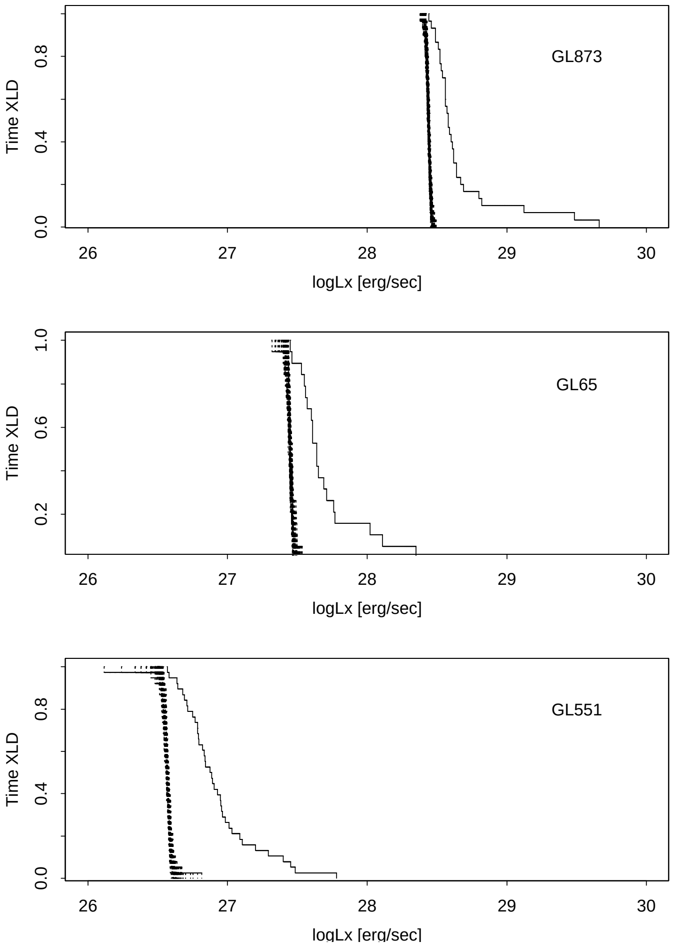

Fig. 3. Cumulative time X-ray luminosity distribution (Time XLD) (single line to right), and simulated Time XLD (lines to the left) from top to bottom: GL873, GL65 and GL551.

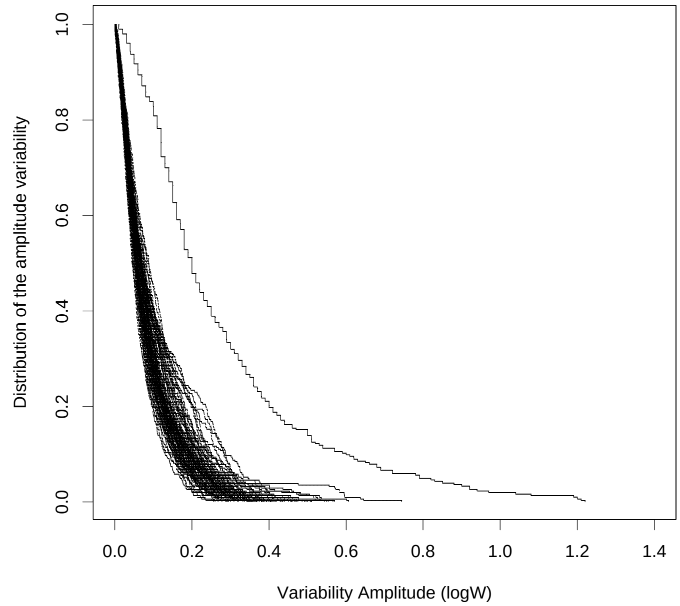

Fig. 4. Normalized cumulative distribution of the amplitude variability (single line to the right) for all our sample together with simulated distributions (lines to the left). W = $L_x/L_{x,min}$ (see Sect. 3.2).

Table 5. The percentage of the observed variance due to statistical fluctuations.

Percentage of the variance due to statistical fluctuations	Number of stars
<1%	6
1–5%	7
5–10%	7
10–20%	4
>20%	3

in the simulated Time XLDs is the largest possible for a constant source, since it is obtained by taking the minimum value for the count rate. The minimum number of photon counts results in the largest statistical uncertainties. If we assume a different value, for example the median value, we would obtain a similar curve with a mean value larger than the previous one but a smaller variance.

For each star we computed the distribution of amplitude variation as the ratio between the observed value of L_x in each temporal segments and the minimum value observed for that star. Since variability does not seem to depend on luminosity, we compute the normalized Time XLD for all stars in our sample. This curve allows us to obtain the variability properties of the nearby M stars population assuming that all nearby M stars belong to the same population as far as X-ray variability is concerned.

The normalized Time XLD (single line to the right) integrated for all our sample star together with simulated distributions (lines to the left) are shown in Fig. 4. Here the fluctuations account for 10% of the observed variance. The distribution gives the fraction of time that an M star spends in a state of a certain flux larger than a given factor of its minimum value. For example, a star spends about half of its time with an $L_x > 1.5 * L_{x,min}$ and 10% of its time with an $L_x > 4 * L_{x,min}$.

In Fig. 5 we compare our normalized cumulative distribution of amplitude variability with the distribution reported for ρ Oph (IPC data, Montmerle et al. 1983) and the one for solar flares in the (2–10) Å range (Drake 1971). Note that in the case of the Sun we are using the relation obtained for flares and in the case of in ρ Oph stars the variability is also attributed to flare events. Both distributions are similar to that of dM stars, suggesting that also the X-ray variations observed in dM stars have a flare-like origin.

If we compare the amplitude distribution function of our sample stars with the spread in X-ray luminosity functions of M stars derived by Barbera et al. (1993) and Schmitt et al. (1995), we find that variability on time scales shorter than a few years may account for only a small fraction of the spread found in the luminosity function. In particular Schmitt et al. (1995) find that the X-ray luminosity distribution function of stars with $8 \leq M_v \leq 15$ is well represented by a log-normal distribution with mean value 27.55 and variance 0.59. The fraction of this

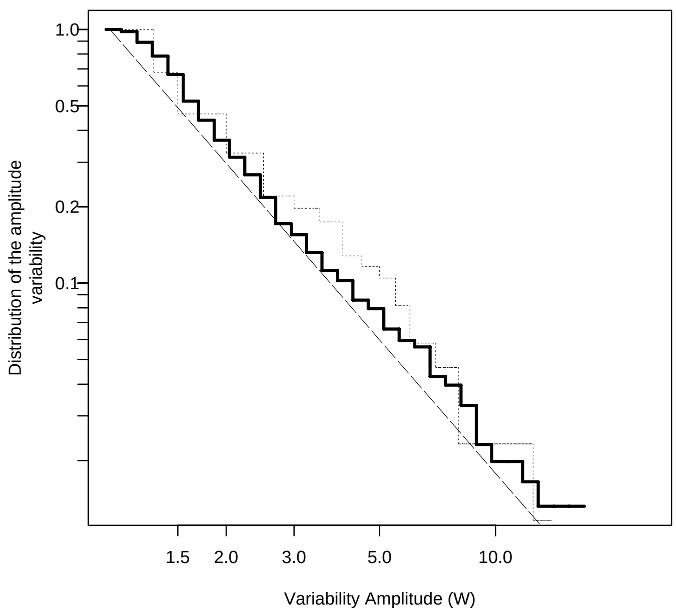

Fig. 5. Normalized cumulative distribution of the amplitude variability of our sample (solid line) in logarithm scale. For comparison we report the analogous distributions for ρ Oph (Montmerle et al. 1983, dotted line) and for solar flares in the (2–10) Å range (Drake 1971, dashed line). W = $L_x/L_{x,min}$ (see Sect. 3.2).

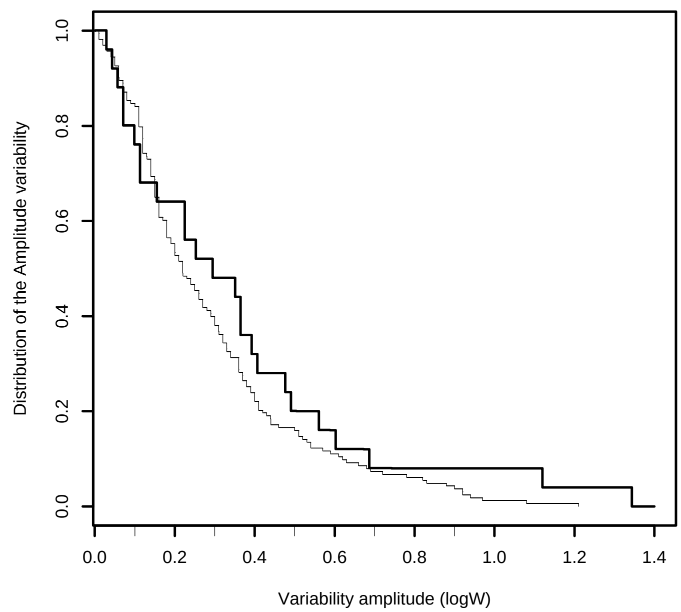

Fig. 6. Normalized cumulative distribution of the amplitude variability of the stars observed both with PSPC and IPC (thick line), and for the same stars but limitedly to PSPC (thin line). W = $L_x/L_{x,min}$ (see Sect. 3.3).

variance due to variability as estimated from the distribution in Fig. 4 is 9% of the total.

We have also verified that choosing a photon count threshold different from the value we have adopted (30 counts), does not affect significantly our results.

3.3. Long term variability

In the soft X-ray band pass the solar X-ray flux varies by about one order of magnitude during the solar cycle (Kreplin et al. 1977, Peres et al. 1999). Solar-like activity cycles have been observed in some late-type stars from optical continuum variations and from chromospheric flux variations (Wilson 1978, Baliunas et al. 1995). So far only a few studies have been carried out in the X-ray bandpass. Combining X-ray data taken with *Einstein* and ROSAT allows us, for the first time, to begin a systematic search of cycles in the stellar coronae. Although the IPC and the PSPC have slightly different bandpasses, the fluxes measured by the two instruments in general present a systematic difference, evaluated as the median of the ratios of the fluxes, of only ∼5%, i.e. 0.02 in $\log(L_x)$. This confirms that the X-ray luminosity functions derived from these two surveys are consistent.

Twenty nine stars in our sample have been observed both with the *Einstein IPC* in 1978–1981, and with ROSAT PSPC between 1990 and 1994. For each star, several data points are available from ROSAT PSPC observations, but only one from IPC data (L_E) (Barbera et al. 1993). In order to reduce the influence of short and medium term variability present in ROSAT PSPC data, we have averaged the latter yielding a single value (L_R) for ROSAT PSPC data. In Fig. 6 we plot the distribution of the X-ray variability observed between the ROSAT and the *Einstein* observations. The amplitude variability is defined by $\log(L_x/L_{x,min})$, where L_x is the higher and $L_{x,min}$, the lower between L_E and L_R. For comparison we show the amplitude distribution obtained for PSPC observations limited to stars which were observed with the IPC and the PSPC. In some cases the IPC observations provide only an upper limits for the flux which results in a lower limit in the PSPC/IPC X-ray luminosity ratio. Therefore, the amplitude distribution is a maximum likelihood distribution (see Sciortino & Micela 1992, Schmitt et al. 1993).

In Fig. 6 the amplitude distribution for a time scale of about 14 years is compared with the distribution computed for time scales of months. The similarity of these distributions indicates that long term variations (similar to the solar cycle), if exist, must be of much smaller amplitudes than the short term variations which dominate the ROSAT X-ray light curves of our sample stars. Incidentally, we note that some stars (e.g. GL206 and GL46), even showing evidence of short term variability, may have an average count rate constant on a six months time scale, just proving the complexity of the scenario of X-ray variability on stars.

We do not find evidence for high amplitude variability on time scales of the order of ten years in M stars. On a larger data base we confirm the results of Schmitt et al. (1995) who investigated a smaller sample of K and M stars. Stern et al. (1995) obtained similar results comparing the *Einstein* and ROSAT data of the Hyades main-sequence stars. They suggest that the lack of strong cyclic activity in young stars indicates that small-scale turbulent magnetic field generation is much more dominant in later stars of Hyades age than the large-scale dynamo that accounts for the Sun's magnetic cycle. It is possible that a similar scenario is valid for all field dM stars.

4. Summary and conclusions

We have presented a systematic analysis of X-ray variability properties of nearby dM stars as observed with ROSAT PSPC. The sample includes 86 pointed observations of 55 distinct stars. Variability is a general property of these stars, independent of the average X-ray luminosity of the stars on all time scales we have explored.

For our sample of nearby dM stars we have generated the time distribution function of the X-ray amplitude variations. The distribution obtained is consistent with the equivalent distribution for solar flares and with the distribution obtained for stars in the ρ Oph star forming region. This suggests that X-ray variability in dM stars is caused by flare-like events.

Our approach allows us to study the statistical properties of variability of dM stars, and is complementary to the individual analysis of a given source. We have evaluated the influence of variability on X-ray distribution function obtained for nearby stars and find that such variability accounts only for a small fraction of the spread in this distribution.

By comparing the present data with published *Einstein* data we find that long term variability (on time scales longer than 10 years), if present, must be of smaller amplitudes than the short term variations observed in the ROSAT X-ray light curves.

Our work suggests that the "quiescent" L_x value is determined by parameters (such as rotation) that do not affect variability. Variability, in fact, does not appear to depend on the quiescent luminosity level, thus raising the question whether variability and luminosity (two different aspects of activity) are decoupled.

The results obtained in our analysis are valid for field dM stars. We expect that a similar investigation of dG stars may provide different results, at least for less active stars similar to our Sun, in which a long term cyclic activity has been clearly detected.

Acknowledgements. The authors acknowledge financial support from ASI (Italian Space Agency), and MURST (Ministero della Università e della Ricerca Scientifica e Tecnologica). We thank F. Reale, and S. Sciortino for their remarks and suggestions and D. Randazzo for significant help in revising the text and the anonymous referee.

References

Ambruster C.W., Sciortino S., Golub L., 1987, ApJS 65, 273
Baliunas S.L., Donahue L., M., Soon W.H., et al., 1995, ApJ 438, 269
Barbera M., Micela G., Sciortino S., Harden F.R.J., Rosner R. 1993, ApJ 414, 846
Collura A., Maggio A., Sciortino S., Vaiana G. S., Rosner R., 1987, ApJ 315, 340
Collura A., Pasquini L., Schmitt J.H.M.M., 1988, A&A 205, 197
Durney B.R., De Young D.S., Roxburgh I.W., 1993, Sol. Phys. 145, 207
Drake J., 1971, Sol. Phys. 16, 152
Eadie W.T., Drijard D., James F.E., Roos M., Sadoulet B., 1971, Statistical Methods in Experimental Physics. North-Holland, Dordrecht
Giacconi R., Branduardi G., Briel U., et al., 1979, ApJ 230, 540
Gliese W., Jahreiss H., 1991, Third Catalogue of nearby stars. Astron. Rech. Inst., Heidelberg
Golub L., 1983, In: Byrne P.B., Rodonò M. (eds.) Activity in Red-Dwarf Stars. Reidel, Dordrecht, p. 83
Haisch B., Schmitt J.H.M.M., 1994, ApJ 426, 716
Kreplin R.W., Dere K.P., Horan D.M., Meekins J.F., 1977, The solar output and its variations. Colorado University Press, 187
Leggett S.K., 1992, ApJS 82, 351
Montmerle T., Koch-Miramond L., Falgarone E., Grindlay J.E., 1983, ApJ 269, 182
Pallavicini R., Tagliaferri G., Stella L., 1990, A&A 228, 403
Peres G., Orlando S., Reale F., Rosner R., Hudson H., 1999, ApJ in press
Pfeffermann E., Briel U., Hippmann H., et al., 1987, Proc. SPIE 733, 519
Raymond J., Smith B.W., 1977, ApJS 35, 429
Rosner R., Golub L., Vaiana G.S., 1985, ARA&A 23, 413
Schmitt J.H.M.M., Kahabka P., Stauffer J., Piters A., 1993, A&A 277, 114
Schmitt J.H.M.M., Fleming T.A., Giampapa M.S., 1995, ApJ 450, 392
Sciortino S., Micela G., 1992, ApJ 388, 595
Siegel S., 1956, Nonparametric Statistics. McGraw-Hill Book Company
Stern R.A., Schmitt J.H.M.M., Kahabka P.T., 1995, ApJ 448, 683
Trümper J., 1992, QJRAS 33, 165
Vaiana G.S., Tucker W.H., 1974, In: Giacconi R., Gursky (eds.) Solar X-ray Emission. Reidel, Dordrecht, p. 169
Vaiana G.S., Davis J.M., Giacconi R., et al., 1973, ApJ 185, L47
Vaiana G.S., Cassinelli J.P., Fabbiano G., et al., 1981, ApJ 245, 163
White N.E., Peacock A., 1988, Mem. Soc. Astron. Ital. 59, 7
Wilson O.C., 1978, ApJ 226, 379
Withbroe G.L., Habbal S.R., Ronan R., 1985, Sol. Phys. 95, 297
Zombeck M.V., Vaiana G.S., Haggerty R., et al., 1978, ApJS 38, 69